Open access • Journal Article • DOI:10.1103/PHYSREVA.31.903

Nonperiodic flow in the numerical integration of a nonlinear differential equation of fluid dynamics — Source link

Edmund X. DeJesus, Charles Kaufman

Published on: 01 Feb 1985 - Physical Review A (Phys Rev A Gen Phys)

Topics: Fluid dynamics, Nonlinear system, Differential equation, Reynolds number and Turbulence

2-1985

Nonperiodic Flow in the Numerical Integration of a Nonlinear Differential Equation of Fluid Dynamics

Edmund X. DeJesus

Charles Kaufman
University of Rhode Island, ckaufman@uri.edu

Citation/Publisher Attribution
DeJesus, E. X., & Kaufman, C. (1985). Nonperiodic flow in the numerical integration of a nonlinear differential equation of fluid dynamics. *Physical Review A, 31*(2), 903-909. doi: 10.1103/PhysRevA.31.903
Available at: http://dx.doi.org/10.1103/PhysRevA.31.903

Nonperiodic flow in the numerical integration of a nonlinear differential equation of fluid dynamics

Edmund X. DeJesus and Charles Kaufman
Department of Physics, University of Rhode Island, Kingston, Rhode Island 02881
(Received 20 April 1984)

Viscous incompressible fluid flow along a flat plate is modeled by the Navier-Stokes equations with appropriate boundary conditions. A series solution is assumed and a set of three nonlinear ordinary differential equations is derived by truncating the series. The Reynolds number appears in these three equations as a parameter. These equations are solved by numerical integration. We show that these solutions exhibit qualitatively different behavior for different values of the Reynolds number of the fluid. The various modes include an asymptotic approach to a time-independent state, laminar (periodic) flow, and turbulence. We give several computer-generated pictures of the various modes.

I. INTRODUCTION

The Orr-Sommerfeld equation provides the classic route for the determination of boundary layer stability of fluid flow along a flat plate.[1-3] More recently, chaotic solutions to differential equations have become a tantalizing possibility for the mathematical description of turbulent flow.[4-8] Here we report on some results of calculations which combine aspects of both approaches. We derive a nonlinear partial differential equation to approximate flow along a flat plate. From this equation we determine a set of three ordinary nonlinear differential equations, and demonstrate that solutions to these equations exhibit both regular and chaotic behavior. We present also some details of this behavior.

II. PROCEDURE

A. Derivation of equations

We begin with the Navier-Stokes equation for viscous flow.[1] Written in terms of the vorticity, these are

$$\rho\frac{d\Omega_k}{Dt}=\mu\frac{\partial^2\Omega_k}{\partial x_l\partial x_l}+\left[\frac{DU_i}{Dt}\epsilon_{ijk}\right]\frac{\partial\rho}{\partial x_j}+\rho\Omega_l\frac{\partial U_k}{\partial x_l}-\rho\Omega_k\theta\ , \tag{1}$$

where Ω_k is kth component of vorticity, t is time, μ is absolute viscosity, x_l is the lth space coordinate, U_k is the kth component of the flow velocity, θ is the divergence of the flow velocity, and k is 1,2,3.

We assume the fluid incompressible, so that the second term on the right-hand side of (1) is zero; also, θ, the divergence of the flow velocity, is zero and the fourth term on the right-hand side of (1) is zero. We retain

$$\rho\frac{D\Omega_k}{Dt}=\mu\frac{\partial^2\Omega_k}{\partial x_l\partial x_l}+\rho\Omega_l\frac{\partial U_k}{\partial x_l}\ . \tag{2}$$

We further assume the flow field U_k to be a basic flow, $\bar{U}_1(x_2)$, with a perturbation of $u_1(x_1,x_2,t)$ and $u_2(x_1,x_2,t)$, i.e.,

$$U_1=\bar{U}_1+u_1\ , \tag{3a}$$

$$U_2=u_2\ , \tag{3b}$$

$$U_3=0\ . \tag{3c}$$

Consider Eq. (2) with $k=3$:

$$\rho\frac{D\Omega_3}{Dt}=\mu\frac{\partial^2\Omega_3}{\partial x_l\partial x_l}+\rho\Omega_l\frac{\partial U_3}{\partial x_l}\ . \tag{4}$$

Using Eq. (3c), $U_3=0$ and the second term on the right-hand side of Eq. (4) is zero. We evaluate Ω_3 in terms of the basic flow and perturbative flow as

$$\begin{aligned}\Omega_3&=-\epsilon_{ij3}\frac{\partial U_i}{\partial x_j}\\&=-\frac{\partial(\bar{U}_1+u_1)}{\partial x_2}+\frac{\partial u_2}{\partial x_1}\\&=\frac{\partial u_2}{\partial x_1}-\frac{\partial u_1}{\partial x_2}-\frac{\partial\bar{U}_1}{\partial x_2}\ ,\\ \Omega_3&=\omega_3-\frac{\partial\bar{U}_1}{\partial x_2}\ ,\end{aligned} \tag{5}$$

where

$$\omega_3\equiv\frac{\partial u_2}{\partial x_1}-\frac{\partial u_1}{\partial x_2}\ .$$

With Ω_3 from Eq. (5), $U_3=0$, and with some rearrangement, Eq. (4) is

$$\left[\frac{\partial}{\partial t}+(\bar{U}_1+u_1)\frac{\partial}{\partial x_1}+u_2\frac{\partial}{\partial x_2}\right]\omega_3$$
$$-\left[\frac{\partial}{\partial t}+(\bar{U}_1+u_1)\frac{\partial}{\partial x_1}+u_2\frac{\partial}{\partial x_2}\right]\frac{\partial \bar{U}_1}{\partial x_2}$$
$$=\frac{\mu}{\rho}\nabla^2\omega_3-\frac{\mu}{\rho}\nabla^2\frac{\partial \bar{U}_1}{\partial x_2}\,. \quad (6)$$

Recall that $\bar{U}_1\equiv\bar{U}_1(x_2)$, so that derivatives of $\bar{U}_1$ with respect to t or x_1 are zero. We rearrange the resultant equation:

$$\frac{\partial\omega_3}{\partial t}+\bar{U}_1\frac{\partial\omega_3}{\partial x_1}+u_1\frac{\partial\omega_3}{\partial x_1}+u_2\frac{\partial\omega_3}{\partial x_2}-u_2\frac{\partial^2\bar{U}_1}{\partial x_2^2}$$
$$=\frac{\mu}{\rho}\nabla^2\omega_3-\frac{\mu}{\rho}\frac{\partial^3\bar{U}_1}{\partial x_3^3}\,. \quad (7)$$

We now introduce a stream function $\Psi=\Psi(x_1,x_2,t)$ to represent the perturbative terms, such that

$$u_1=\frac{\partial\Psi}{\partial x_2}\,, \quad (8a)$$
$$u_2=-\frac{\partial\Psi}{\partial x_1}\,, \quad (8b)$$
$$\omega_3=-\nabla^2\Psi\,. \quad (8c)$$

Using Eqs. (8) in Eq. (7) gives

$$-\frac{\partial}{\partial t}\nabla^2\Psi-\bar{U}_1\frac{\partial}{\partial x_1}\nabla^2\Psi+\frac{\partial^2\bar{U}_1}{\partial x_2^2}\frac{\partial\Psi}{\partial x_1}$$
$$=\frac{-\mu}{\rho}\nabla^4\Psi+\left[\frac{\partial\Psi}{\partial x_2}\frac{\partial}{\partial x_1}\nabla^2\Psi-\frac{\partial\Psi}{\partial x_1}\frac{\partial}{\partial x_2}\nabla^2\Psi\right]$$
$$-\frac{\mu}{\rho}\frac{\partial^3\bar{U}_1}{\partial x_2^3}\,. \quad (9)$$

To simplify the form of Eq. (9) we make the following substitutions: x for x_1, y for x_2, U for $\bar{U}_1$, U_{yy} for $\partial^2\bar{U}_1/\partial x_2^2$, U_{yyy} for $\partial^3\bar{U}_1/\partial x_2^3$, Ψ_x for $\partial\Psi/\partial x_1$, Ψ_y for $\partial\Psi/\partial x_2$. This simplification gives

$$-\frac{\partial}{\partial t}\nabla^2\Psi-U\frac{\partial}{\partial x}\nabla^2\Psi+U_{yy}\Psi_x+\frac{\mu}{\rho}\nabla^4\Psi$$
$$+\left[\Psi_x\frac{\partial}{\partial y}-\Psi_y\frac{\partial}{\partial x}\right]\nabla^2\Psi+\frac{\mu}{\rho}U_{yyy}=0\,. \quad (10)$$

We wish to render Eq. (10) dimensionless. We make the assumption that flow is restricted (in the y direction) to a boundary layer of thickness δ.[1,9] We further assume that the free-stream velocity is U_0. With these assumptions we obtain the dimensionless equation

$$-\left[\frac{\partial}{\partial t}\nabla^2\Psi+U\frac{\partial}{\partial x}\nabla^2\Psi\right]+U_{yy}\frac{\partial\Psi}{\partial x}+\frac{1}{R}\nabla^4\Psi$$
$$+\left[\Psi_x\frac{\partial}{\partial y}-\Psi_y\frac{\partial}{\partial x}\right]\nabla^2\Psi\frac{1}{R}U_{yyy}=0\,, \quad (11)$$

where $R\equiv\rho\delta U_0/\mu$ is identified as the Reynolds number. (Note that by neglecting terms nonlinear in Ψ and assuming U_{yyy} vanishes, Eq. (11) can be truncated. Assuming that Ψ is of the form $\Psi=\phi(y)\exp[i\alpha(x-ct)]$ in this truncated equation then yields the Orr-Sommerfeld equation. Equation (11) is implicit in the standard derivation of the Orr-Sommerfeld equation, but does not explicitly appear in standard references on the subject.[9])

1. *Choosing the stream function* Ψ

It is difficult to choose a stream function, $\Psi(x,y,t)$, which preserves the nonlinear character of Eq. (11). After examining many possibilities, we have chosen

$$\Psi=\Psi(x,y,t)=-\frac{A}{l^2}\cos(ly)-\frac{B}{k^2}\cos(kx)$$
$$-\frac{2C}{k^2+l^2}\sin(ly)\sin(kx)\,, \quad (12)$$

where $A=A(t)$, $B=B(t)$, $C=C(t)$, and k,l are positive real constants. This choice was suggested by a stream function used by Lorenz in his paper "Maximum Simplification of the Dynamic Equations."[10]

Using Eq. (12) in Eq. (11) gives

$$-\dot{A}\cos(ly)-\frac{l^2}{R}A\cos(ly)-\dot{B}\cos(kx)-\frac{k^2}{R}B\cos(kx)-2\dot{C}\sin(ly)\sin(kx)-2\frac{(k^2+l^2)}{R}C\sin(ly)\sin(kx)$$
$$+AB\left[\frac{k^2-l^2}{kl}\right]\sin(kx)\sin(ly)+2BC\frac{l^3}{k(k^2+l^2)}\cos(ly)-BC\frac{l^3}{k(k^2+l^2)}\cos(ly)\cos^2(kx)$$
$$+2AC\frac{-k^3}{l(k^2+l^2)}\cos(kx)-2AC\frac{-k^3}{l(k^2+l^2)}\cos(kx)\cos^2(ly)+Ukb\sin(kx)$$
$$+U_{yy}\frac{B}{k}\sin(kx)-2kCU\sin(ly)\sin(kx)-U_{yy}\frac{2k}{k^2+l^2}C\sin(ly)\cos(kx)+\frac{1}{R}U_{yyy}=0\,. \quad (13)$$

2. *Choosing the flow function U*

The flow function U is a function of y only. The boundary conditions of flow along a flat plate suggest that U should be small for y near zero. Also, U should approach U_0 as y approaches the boundary layer thickness, δ. (This latter restriction can be achieved through the use of a multiplicative constant.) These restrictions still allow considerable freedom in choosing U. We chose (and justify our choice in the Appendix)

$$U_{yy}=\frac{m}{\sin(ly)} . \tag{14}$$

It is our intention to keep only those terms of Eq. (13) that are like the terms appearing in Ψ, Eq. (12),[6,11] namely, multiples of $\cos(ly)$, $\cos(kx)$, and $\sin(ly)\sin(kx)$. Therefore we make the trigonometric substitutions $1-\sin^2(kx)$ for $\cos^2(kx)$ and $1-\sin^2(ly)$ for $\cos^2(ly)$ in Eq. (13). We also substitute Eq. (14) in Eq. (13), noting that U and U_{yy} will give rise to terms that will not be kept. The resulting equation is

$$\cos(ly)\left[-\dot{A}-\frac{l^2}{R}A+BC\frac{2l^3}{k(k^2+l^2)}\right]+\cos(kx)\left[-\dot{B}-\frac{k^2}{R}B+AC\left[\frac{-2k^3}{l(k^2+l^2)}\right]-C\frac{2km}{k^2+l^2}\right]$$
$$+\sin(ly)\sin(kx)\left[-2\dot{C}-2\frac{(k^2+l^2)}{R}C+AB\frac{(k^2-l^2)}{kl}\right]=0 . \tag{15}$$

In Eq. (15), the terms $\cos(ly)$, $\cos(kx)$, and $\sin(ly)\sin(kx)$ are linearly independent, so that the coefficients of these terms must separately equal zero.[12] This yields

$$\dot{A}=\frac{-l^2}{R}A+BC\left[\frac{2l^3}{k(k^2+l^2)}\right] , \tag{16a}$$

$$\dot{B}=\frac{-k^2}{R}B+AC\left[\frac{-2k^3}{l(k^2+l^2)}\right]+C\left[\frac{-2km}{k^2+l^2}\right] , \tag{16b}$$

$$\dot{C}=-\frac{(k^2+l^2)}{R}C+AB\left[\frac{k^2-l^2}{2kl}\right] . \tag{16c}$$

Equations (16) can also be written as

$$\dot{A}=d_1A+d_2BC+d_3B , \tag{17a}$$

$$\dot{B}=e_1B+e_2AC+e_3C , \tag{17b}$$

$$\dot{C}=f_1C+f_2AB+f_3A , \tag{17c}$$

where

$$d_1=-\frac{l^2}{R},\quad d_2=\frac{2l^3}{k(k^2+l^2)},\quad d_3=0 ,$$
$$e_1=-\frac{k^2}{R},\quad e_2=\frac{-2k^3}{l(k^2+l^2)},\quad e_3=\frac{-2km}{k^2+l^2} ,$$
$$f_1=\frac{-(k^2+l^2)}{R},\quad f_2=\frac{k^2-l^2}{2kl},\quad f_3=0 .$$

Equations (17) are the equations we integrated numerically.

The approximations leading to these equations have been severe, and much of the content of Eq. (11) may have been lost thereby. We do not expect Eqs. (17) to describe real flow to high precision. However, the nonlinearity and dependence on Reynolds number do remain, and we proceed to numerically integrate these equations, with an eye more toward qualitative than quantitative description of real flow.

B. Numerical integration of equations (Ref. 6).

Given A_n,B_n,C_n we compute $\dot{A}_i,\dot{B}_i,\dot{C}_i$:

$$\dot{A}_i=d_1A_n+d_2B_nC_n ,$$
$$\dot{B}_i=e_1B_n+e_2A_nC_n+e_3C_n , \tag{18}$$
$$\dot{C}_i=f_1C_n+f_2A_nB_n .$$

From $\dot{A}_i,\dot{B}_i,\dot{C}_i$ and the time interval Δt we can compute the midpoint $A_{(n+1)},B_{(n+1)},C_{(n+1)}$:

$$A_{(n+1)}=A_n+\dot{A}_i\Delta t ,$$
$$B_{(n+1)}=B_n+\dot{B}_i\Delta t , \tag{19}$$
$$C_{(n+1)}=C_n+\dot{C}_i\Delta t .$$

Now we compute $\dot{A}'_i(A_{(n+1)},B_{(n+1)},C_{(n+1)})$, $\dot{B}'_i(A_{(n+1)},B_{(n+1)},C_{(n+1)})$, $\dot{C}'_i(A_{(n+1)},B_{(n+1)},C_{(n+1)})$:

$$\dot{A}'_i=d_1A_{(n+1)}+d_2B_{(n+1)}C_{(n+1)} ,$$
$$\dot{B}'_i=e_1B_{(n+1)}+e_2A_{(n+1)}C_{(n+1)}+e_3C_{(n+1)} , \tag{20}$$
$$\dot{C}'_i=f_1C_{(n+1)}+f_2A_{(n+1)}B_{(n+1)} .$$

Lastly we compute the new point A_{n+1},B_{n+1},C_{n+1}:

$$A_{n+1}=A_n+\frac{\Delta t}{2}(\dot{A}_i+\dot{A}'_i) ,$$
$$B_{n+1}=B_n+\frac{\Delta t}{2}(\dot{B}_i+\dot{B}'_i) , \tag{21}$$
$$C_{n+1}=C_n+\frac{\Delta t}{2}(\dot{C}_i+\dot{C}'_i) .$$

Equations (18)—(21) are the algorithm we used to numerically integrate Eqs. (17).

To preserve the physical validity of the flow characterized by Eqs. (17), some care must be taken in choosing values for the constants k, l, and m. From Schlicting's discussion of a turbulent boundary layer[9] we use the empirical result that the minimum wavelength of the dis-

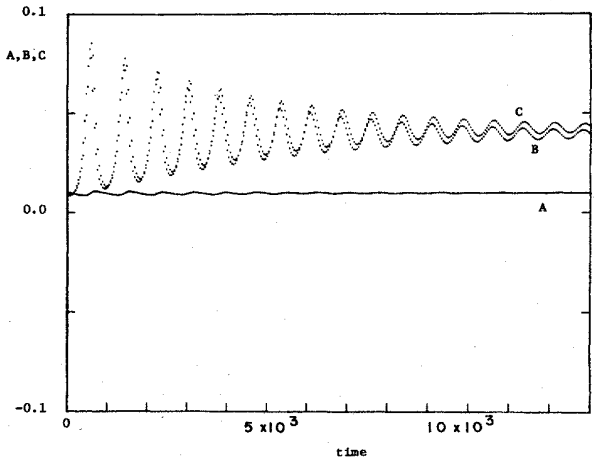

FIG. 1. A,B,C, vs time for $R=10$. Time interval between points shown is 40 units.

turbance be about 6δ, i.e., the wavelength of the disturbance is much larger than the thickness of the boundary layer. In our formulation, k and l play the part of wave numbers [as in the terms $\cos(ly)$, $\cos(kx)$, and $\sin(ly)\sin(kx)$] so that we have the restriction:

$$k,l<1\ .$$

In addition, we impose the further restriction that $k^2>l^2$ so that $f_2>0$ in Eqs. (17). As a result, analysis of the eigenvalues of Eqs. (17) is simplified. Lastly our choice, and justification, of the flow function U require $l\ll 1$ and $n>-l$.

For our study we chose $k=0.62$, $l=0.07$, $m=-0.064$. We used $A=0.01$, $B=0.01$, $C=0.01$ as the initial point of the integration; Δt was 1.

We used double-precision advanced BASIC on the IBM Personal Computer for calculations and graphic results. We also used double-precision FORTRAN on the University of Rhode Island NAS 7000N mainframe computer for calculations and graphic results.

Typical integrations were carried out for 5000 time units, and we estimated the precision of the numerical calculations by studying the effect of reducing the time step Δt. After a time 5000 units, $B(5000)$ for $\Delta t=1$ differed from $B(5000)$ for $\Delta t=\frac{1}{10}$, by about 0.1%.

III. RESULTS

We observed a wide range of qualitative behavior of the solutions of Eqs. (19) corresponding to a range of values of R. For $R<15.5914$, we observed the solutions A,B,C to oscillate regularly (see Fig. 1), the amplitude of oscillations decayed, and the solutions A,B,C approached a

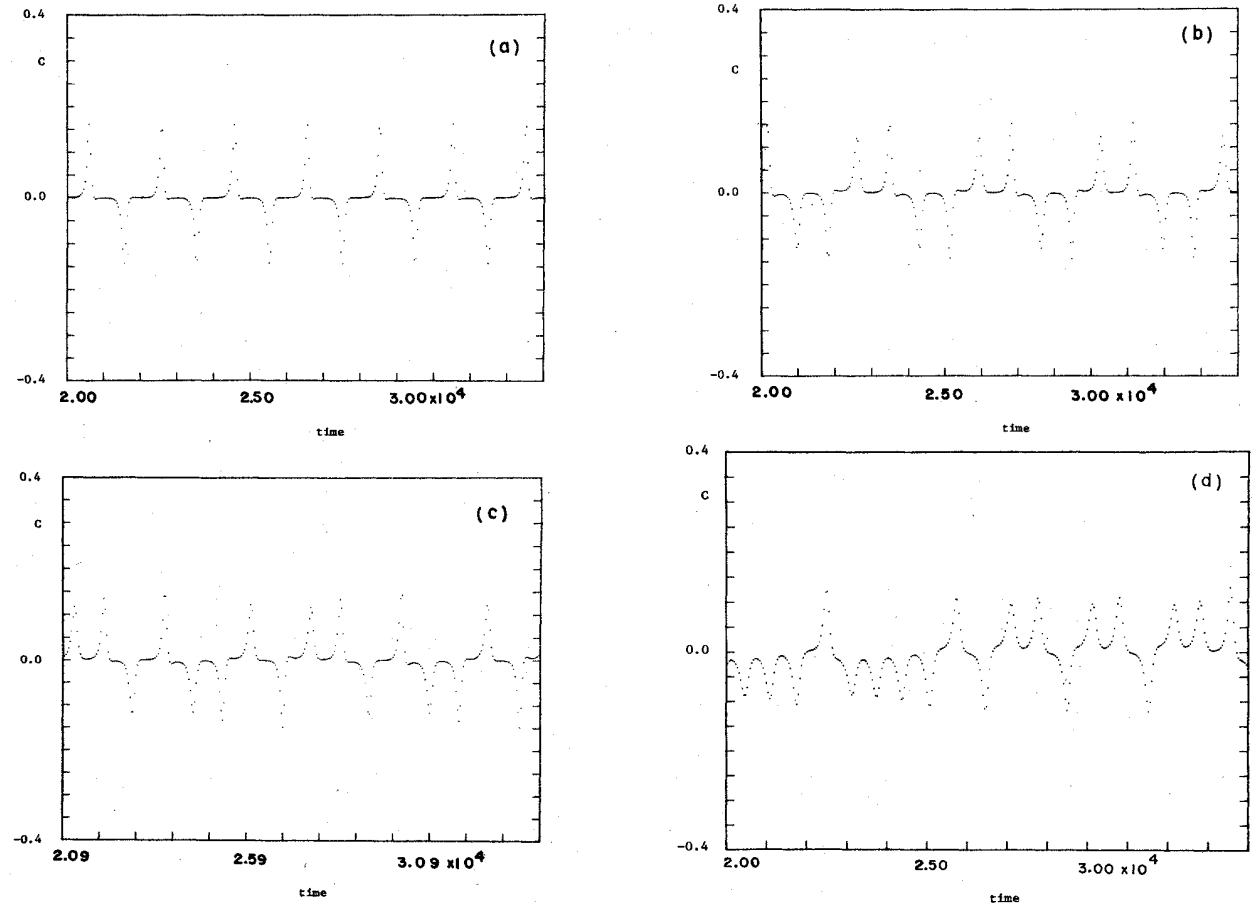

FIG. 2. C vs time for several values of R. Time interval between points shown is 40 units. (a) $R=16$, 4-cycle; (b) $R=22$, 8-cycle; (c) $R=23.4$, 16-cycle; (d) $R=40$, chaotic.

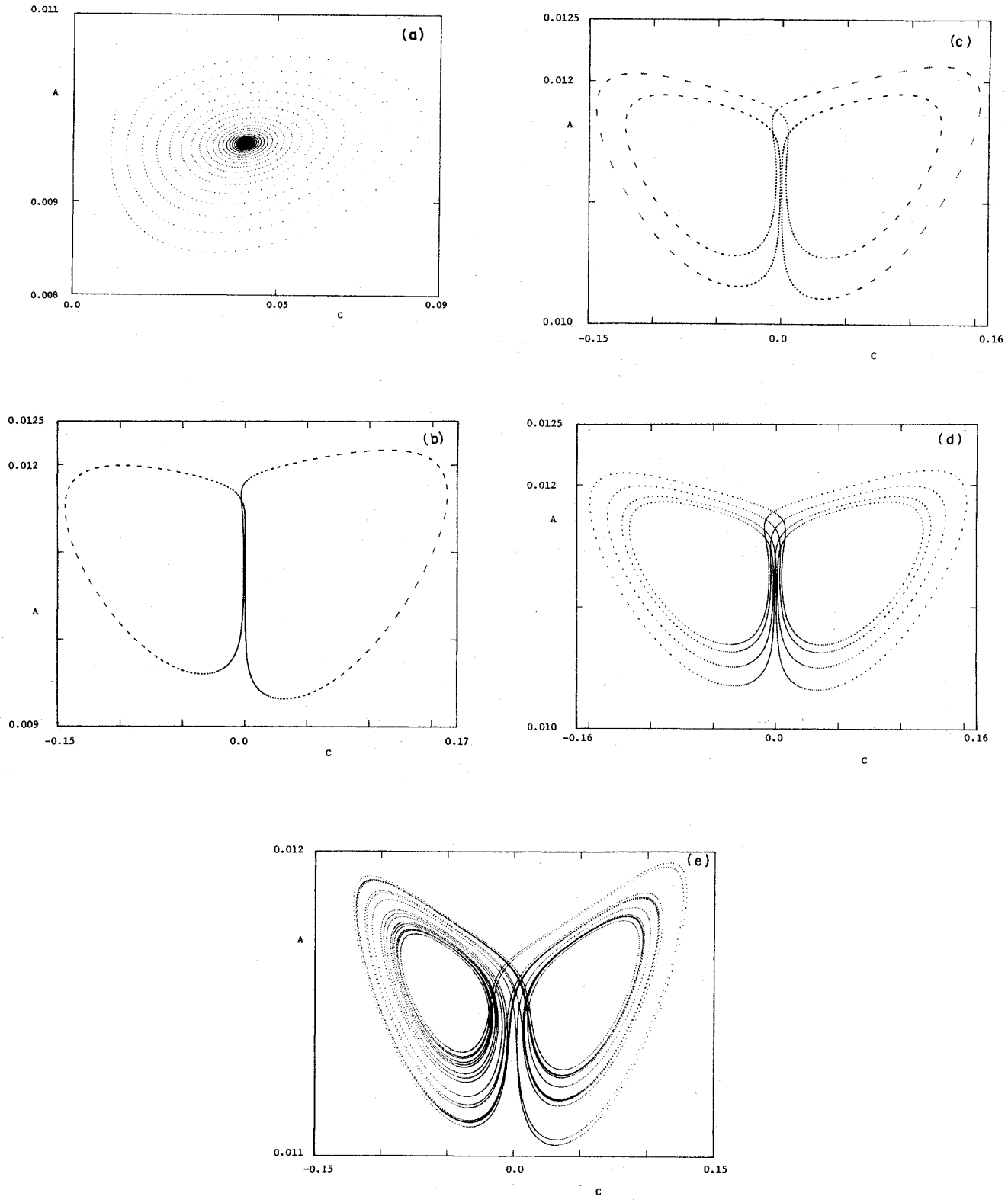

FIG. 3. A vs C for several values of R. Time interval between points shown is 10 units, except in (e), where it is 2 units. (a) $R=10$; (b) $R=16$, 4-cycle; (c) $R=22$, 8-cycle; (d) $R=23.4$, 16-cycle; (e) $R=40$, chaotic.

fixed point. For $15.5914 < R < 18$, the solutions oscillate regularly [see Fig. 2(a)], the amplitude does not decay, and the oscillations appear to form a stable 4-cycle (see the following). For $18 < R < 21$, the solutions oscillate irregularly, the amplitude does not decay, and the oscillations appear to be changing from a 4-cycle to an 8-cycle. For $21 < R < 23$, the solutions oscillate regularly [see Fig. 2(b)], the amplitude does not decay, and the oscillations appear to form a stable 8-cycle (see the following). For $R = 23.4$, the solutions oscillate regularly [see Fig. 2(c)], the amplitude does not decay, and the oscillations appear to form a stable 16-cycle. For $R = 40$, the solutions oscillate irregularly [see Fig. 2(d)], the amplitude does not decay, but varies over a wide range, and the oscillations appear to be chaotic (see the following).

Our judgment as to whether the oscillations are stable n-cycles or chaotic derives from considerations of two types of information: the trajectory of the solution in A,B,C space, and the Poincaré section of that trajectory with a plane, $A = \text{const}$.

Figures 3(a)—3(e) show "three-dimensional" portraits of the trajectories of the solutions in A,B,C space. Figure 3(a) shows the spiraling decay of the solutions toward a fixed point for $R = 10$. Figure 3(b) shows that the trajectory for $R = 16$ is stable and consists of two lobes. Figure 3(c) shows that the trajectory for $R = 22$ is stable and consists of four lobes. Figure 3(d) shows that the trajectory for $R = 23.4$ is stable and consists of eight lobes. Figure 3(e) shows that the trajectory for $R = 40$ is not stable and consists of many lobes of various sizes.

In the nonmenclature of mappings, a mapping is said to be an "n-cycle" if it takes n applications of the mapping to get back to the original point. For instance, a 4-cycle would consist of four points; point 1 would map into point 2, point 2 into point 3, point 3 into point 4, and point four back into point 1. Thus, a 4-cycle takes four steps to return to the original point. Trajectories such as those traced by these solutions do not have such a simple structure. It is useful to take the intersection of this three-dimensional trajectory with a two-dimensional surface. The resulting set of intersection points is known as a Poincaré section or Poincaré map, and gives information about the periodicity of the trajectory.[6,11,13]

For the two-dimensional surface we chose the plane

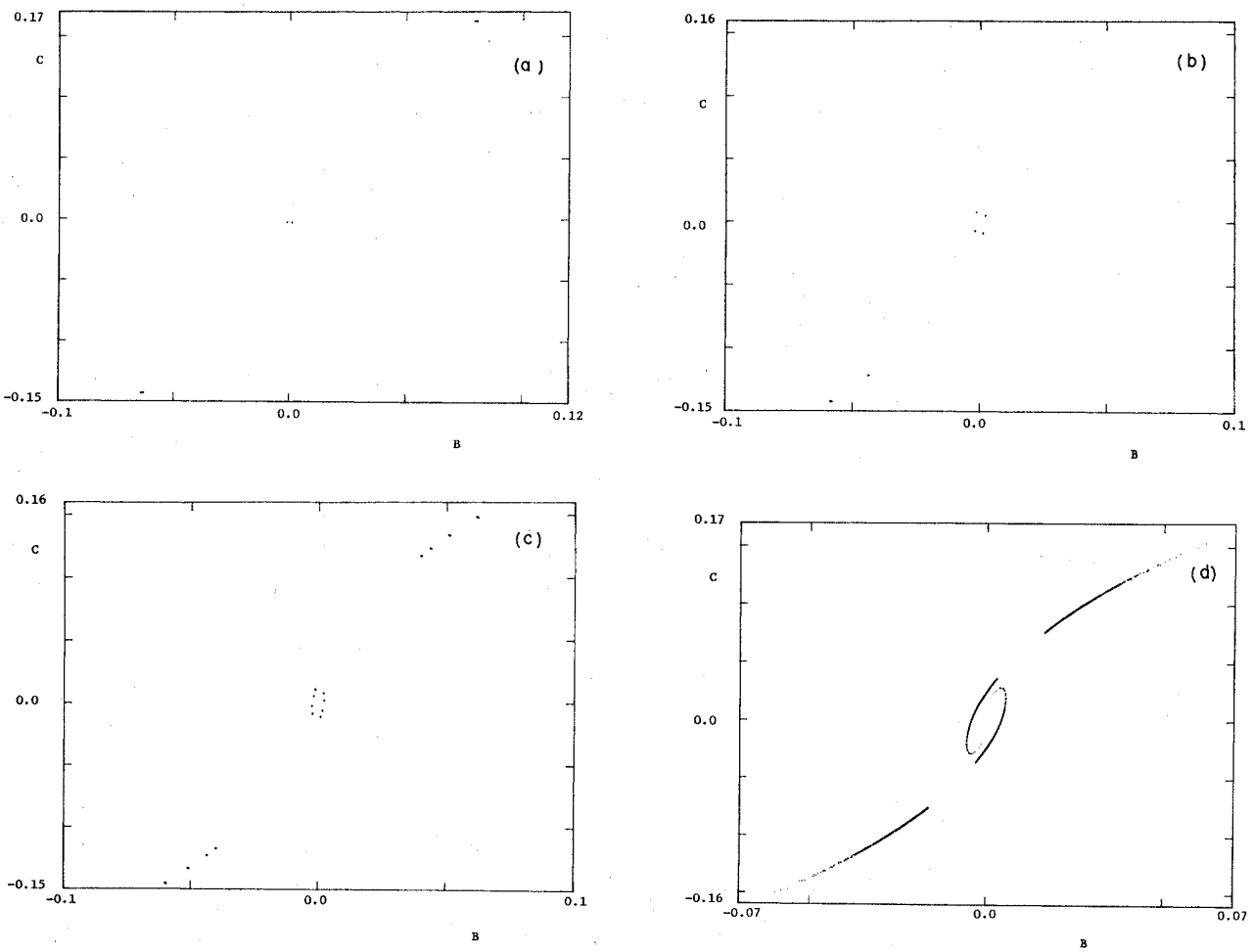

FIG. 4. Intersection of the trajectory with the plane $A = 0.0116$. (a) $R = 16$, 4-cycle, $2\times10^4 < t < 5\times10^4$; (b) $R = 22$, 8-cycle, $2\times10^4 < t < 5\times10^4$; (c) $R = 23.5$, 16-cycle, $2\times10^4 < t < 2\times10^5$; (d) $R = 40$, chaotic, $2\times10^4 < t < 2\times10^5$.

$A=0.0116$. As might be expected, each lobe of a trajectory strikes this plane in two points. For $R=16$, the trajectory of two lobes strikes the plane in four points; thus, $R=16$ is a 4-cycle [Fig. 4(a)]. For $R=22$, the trajectory of four lobes strikes the plane in eight points; thus, $R=22$ is an 8-cycle [Fig. 4(b)]. For 23.4, the trajectory of eight lobes strikes the plane in sixteen points; thus, $R=23.4$ is a 16-cycle [Fig. 4(c)]. For $R=40$, the many lobes strike the plane in many points; the trajectory and the intersection points do not repeat; thus, $R=40$ is nonperiodic, or chaotic [Fig. 4(d)].

IV. CONCLUSIONS

The simple mathematical model of a fluid dynamical system gives rise to equations whose numerical solutions behave in qualitatively different ways. This behavior includes decay to constant values, regular oscillation, and chaos. The authors believe these different behaviors resemble the flow of fluids under different circumstances, viz., fluid motion dissipating due to viscous forces, laminar fluid flow, and turbulent flow.

Moon *et al.*[8] have made a similar study of another equation of fluid dynamics, the Ginzburg-Landau equation. They find periodic and chaotic regimes as the control parameter is varied, just as we do. In addition, the transition to turbulence in their case seems to proceed via the "three-frequency scenario" of Newhouse *et al.* In other work we will attempt to determine the predicted fluid velocities and their spectra from the functions A,B,C, and from there, to determine which, if any, of the competing paths to chaos[14] our model chooses.

ACKNOWLEDGMENTS

The authors wish to thank Dr. Leonard Kahn and Dr. J. Scott Desjardins for many helpful discussions, as well as for the use of Dr. Kahn's Apple computer. One of us (E.X.D.) wishes to acknowledge the support of the International Business Machines Corporation during his educational leave of absence.

APPENDIX: CHOICE OF FLOW FUNCTION U

The choice of flow function U is crucial to the behavior of the mathematically modeled dynamical system. Therefore, the flow function was chosen mainly for its physical relevance and for the mathematical advantage it offered. This advantage was realized in that certain terms are discarded and one term retained as a result of our choice, namely:

$$U_{yy}=\frac{m}{\sin(ly)} .$$

We justify our choice as follows. For $ly \ll 1$, $\sin(ly)\approx ly$, so that

$$U_{yy}\approx \frac{m}{l}\frac{1}{y} .$$

Upon integration with respect to y:

$$U_y \approx \frac{m}{yl}(\ln|y|+C_1) .$$

Upon second integration with respect to y:

$$U\approx \frac{m}{l}(-y+y\ln|y|+C_1y+C_2) .$$

According to our boundary conditions

$$U(y)\to 0 \quad \text{as } y\to 0$$

and

$$U(y)\to 1 \quad \text{as } y\to 1 .$$

From the first condition, we deduce that $C_2=0$. From the second, we deduce that $C_1=1+l/m$. We also desire that U reach its maximum value for $y\geq 1$. This implies $C_1\leq 0$. From the conditions that $U(1)=1$ and $C_1\leq 0$ and $l>0$, we deduce that

$$0>m\geq -l .$$

[1]J. O. Hinze, *Turbulence,* 2nd ed. (McGraw-Hill, New York, 1975).
[2]S. I. Pai, *Viscous Flow Theory* (Van Nostrand, Princeton, 1956), Vol. 1.
[3]J. R. Radbill and G. A. McCue, *Quasilinearization and Nonlinear Problems in Fluid and Orbital Mechanics* (Elsevier, New York, 1970).
[4]V. Franceschini, Physica (Utrecht) **6D**, 285 (1983).
[5]L. P. Kadanoff, Physics Today **36** (12), 46 (1983).
[6]E. N. Lorenz, J. Atmos. Sci. **20**, 130 (1963).
[7]J. B. McLaughlin and P. C. Martin, Phys. Rev. A **12**, 186 (1974).
[8]H. T. Moon, P. Huerre, and L. G. Redekopp, Phys. Rev. Lett. **49**, 458 (1982); Physica (Utrecht) **7D**, 135 (1983).
[9]H. Schlichting, *Boundary Layer Theory,* 7th ed. (McGraw-Hill, New York, 1979).
[10]E. N. Lorenz, Tellus **12**, 242 (1960).
[11]D. A. Russell and E. Ott, Phys. Fluids **24**, 1976 (1981).
[12]E. Butkov, *Mathematical Physics* (Addison-Wesley, Reading, Mass., 1968).
[13]G. D. Birkhoff, *Dynamical Systems* (American Mathematical Society, Providence, 1966).
[14]J. P. Eckmann, Rev. Mod. Phys. **53**, 643 (1981).